

Crown-linked dipyridylamine-triazine ligands and their spin-crossover iron(II) derivatives: magnetism, photomagnetism and cooperativity.

Hayley S. Scott,^a Tamsyn M. Ross,^a Nicholas F. Chilton,^{a,b} Ian A. Gass,^a Boujemaa Moubaraki,^a Guillaume Chastanet,^c Nicolas Paradis,^c Jean-François Létard,^c Kuduva R. Vignesh,^d Gopalan Rajaraman,^d Stuart R. Batten,^a and Keith S. Murray^{a*}

ESI-Supporting Information

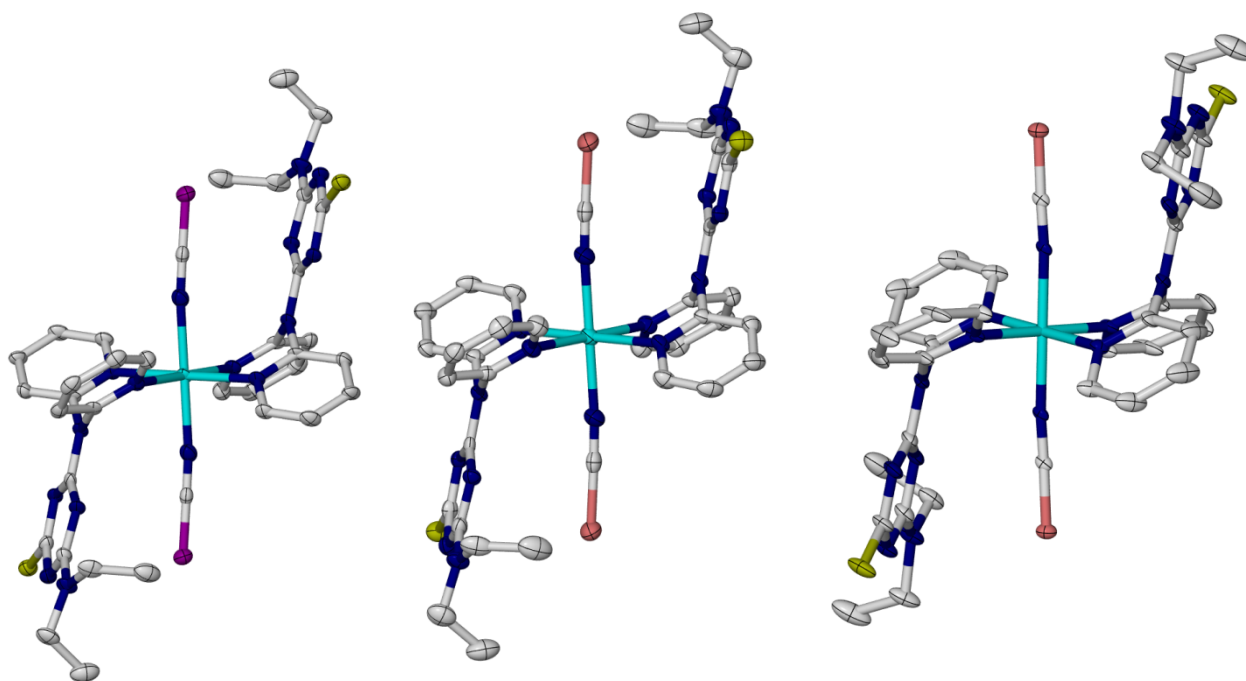


Fig. S1 Structure of the L^1 family of complexes **1-3**, showing the orientation of the diethylamine portion of L^1 . Complexes **1** (left) and **2** (middle) 50% ellipsoids, complex **3** (right) 20% ellipsoids. H atoms omitted for clarity. Nitrogen, dark blue; X (X = S(**1**), Se(**2**), BH₃(**3**)), purple; chlorine, green; Fe^{II}, turquoise.

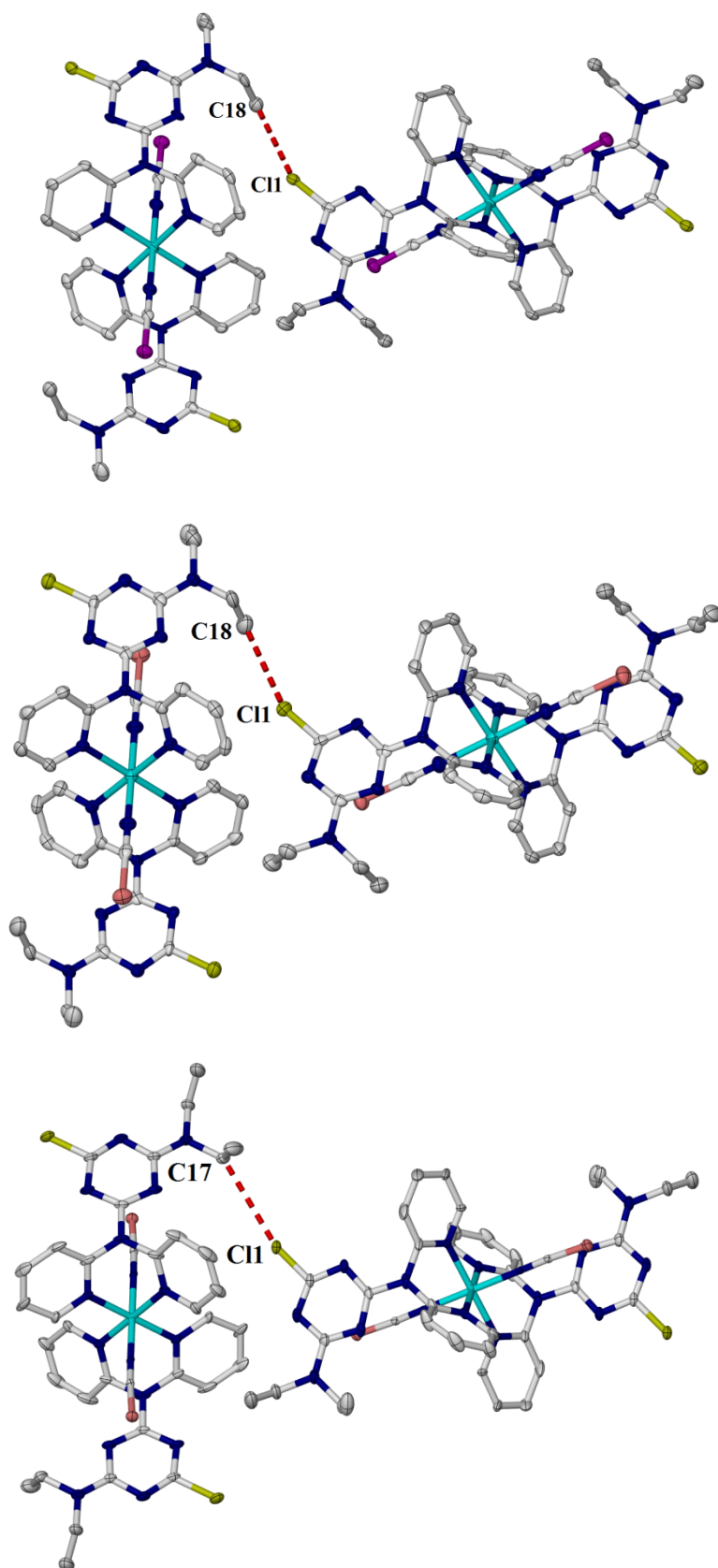


Fig. S2 Structure of the L^1 family of complexes **1**(top), **2**(middle) and **3**(bottom) showing the C-H...Cl contacts as a dashed red line. Complexes **1** and **2** 50% ellipsoids, complex **3** 20% ellipsoids. H atoms omitted for clarity. Nitrogen, dark blue; X (X = S(**1**), Se(**2**), BH₃(**3**)), purple; chlorine, green; Fe^{II}, turquoise.

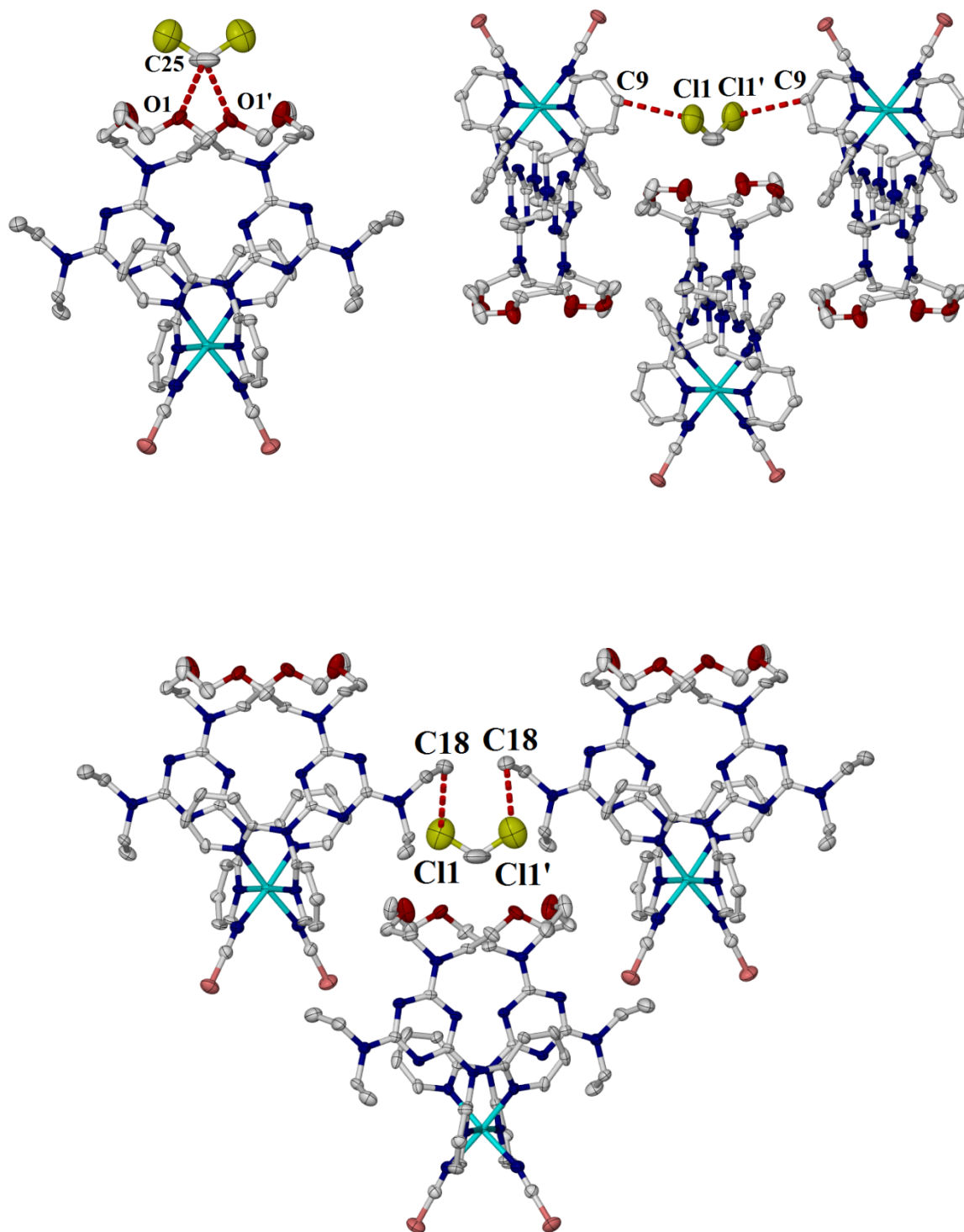


Fig. S3 Structure of **6** showing C-H...O (top left) and C-H...Cl (top right and bottom) contacts as a dashed red line. Complexes **6** shown with 50% ellipsoids. H atoms omitted for clarity. Nitrogen, dark blue; boron, pink; chlorine, green; Fe^{II}, turquoise.

Table S1. Intermolecular interactions lengths (Å) and angles (°) for complexes **1-3** and **6**.

Complex	<i>D-H...A</i>	<i>D-H</i>	<i>H...A</i>	<i>D...A</i>	<i>D-H...A</i>
1	C18-H18B...C11	0.980	2.814	3.415	120.25
2	C18-H18A...C11	0.980	2.782	3.401	121.76
3	C17-H17A...C11	0.990	2.981	3.689	129.38
6	C25-H25B...O1	0.990	2.603	3.425	140.51
6	C9-H9...C11	0.950	2.832	3.690	150.70
6	C18-H18A...C11	0.980	2.835	3.661	142.51

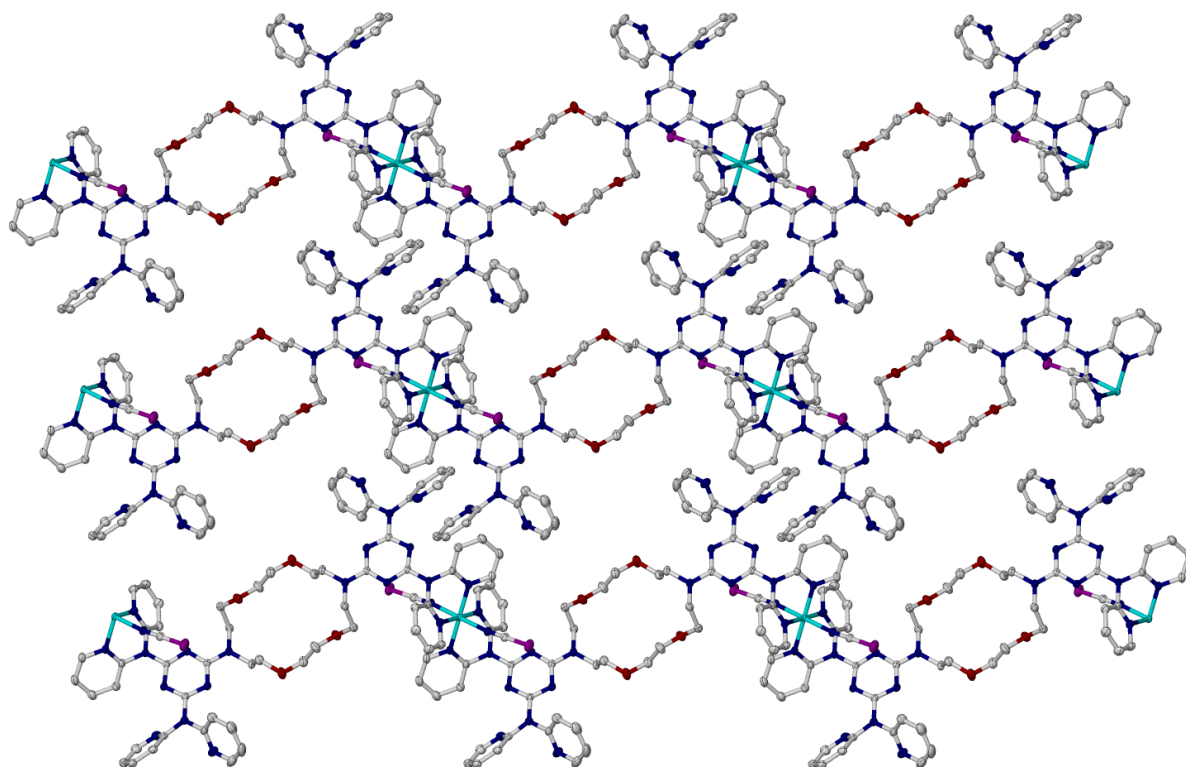


Fig. S4 Packing of **7** (isotstructural to **8**).

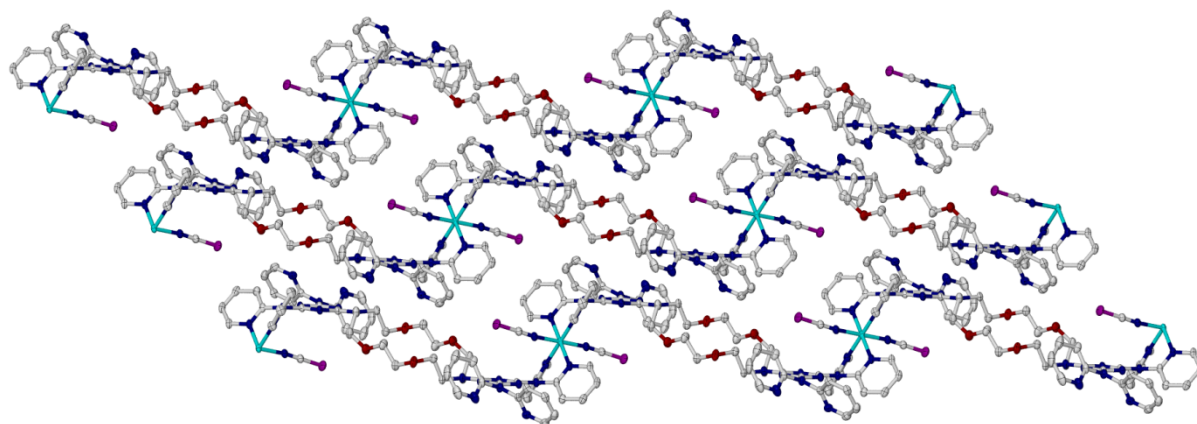


Fig. S5 Packing of **7** (isostructural to **8**).

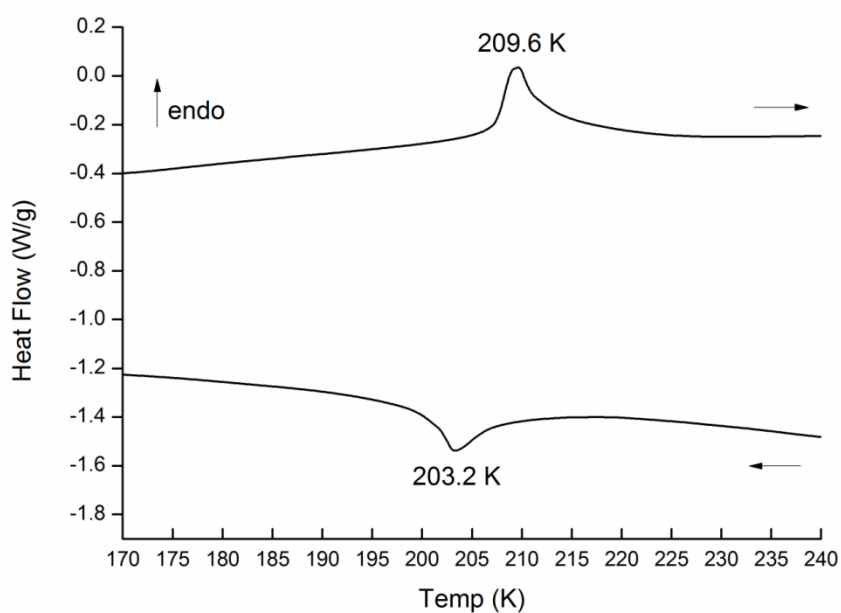


Fig. S6 The differential scanning calorimetric measurement for a single heating and cooling cycle of **3** between 170 K and 240 K. The arrows indicate the cycle direction with the endothermic peaks pointing upwards as indicated.

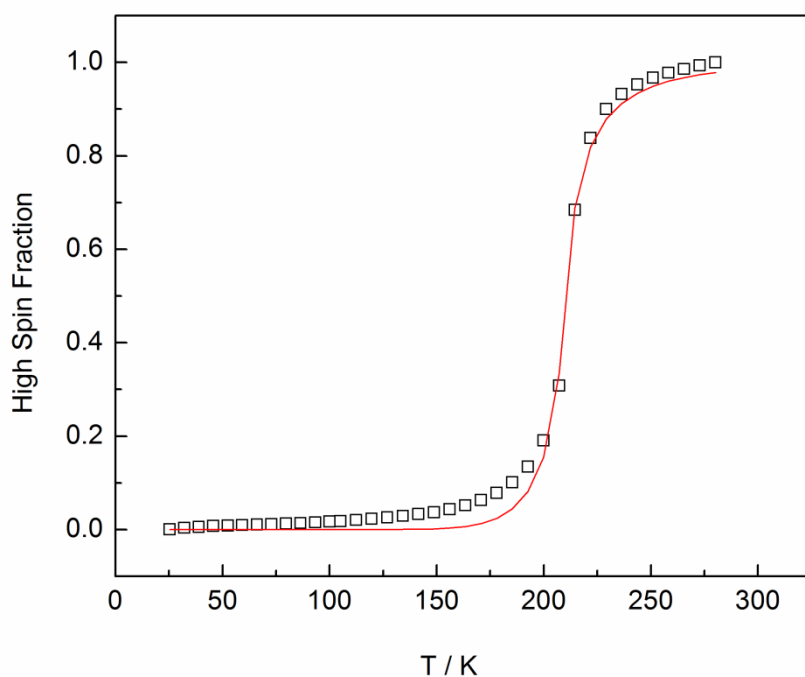


Fig. S7 Plot of high-spin fraction, vs. temperature for complex **3**, where the red line is the best fit to the Slichter-Drickamer mean-field model (eqn. (1) in script) and the ΔH and ΔS and Γ values given in the script. The LS $\chi_M(\text{TIP}; 2^{\text{nd}}$ order Zeeman) contribution (see Fig. 6) has not been included.

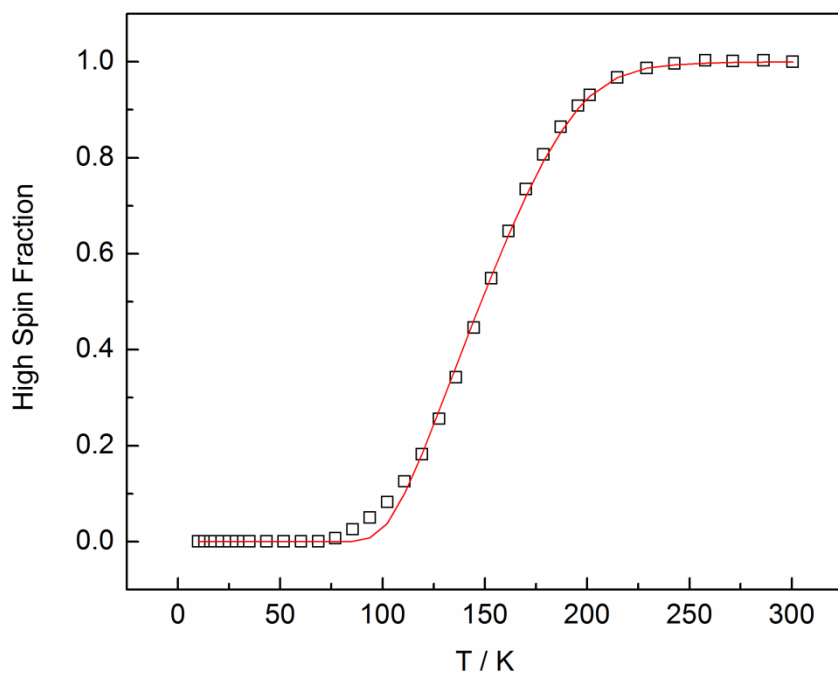


Fig. S8 Plot of high-spin fraction, vs. temperature for complex **6**, where the red line is the best fit to the Slichter-Drickamer mean-field model (eqn. (1) in script) and the ΔH and ΔS and Γ values given in the script. The LS $\chi_M(\text{TIP}; 2^{\text{nd}}$ order Zeeman) contribution (see Fig. 8) has not been included.

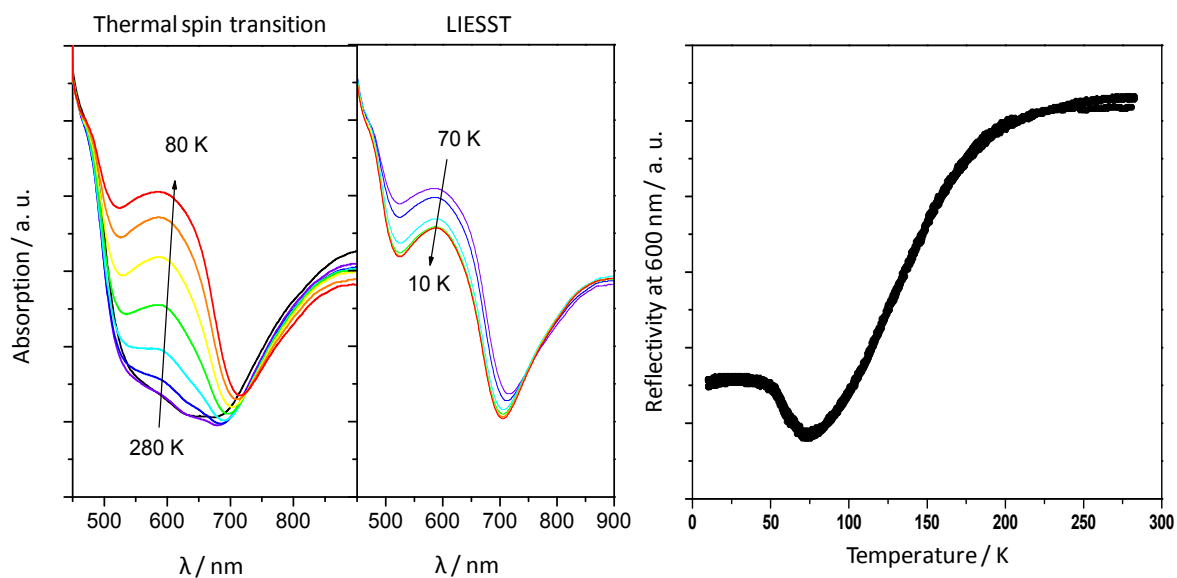


Fig. S9 Thermal dependence of the absorption spectra under light irradiation (left) and intensity of the reflectivity signal at 600 nm (right) for cis-[Fe^{II}(L²)(NCSe)₂], **5**.

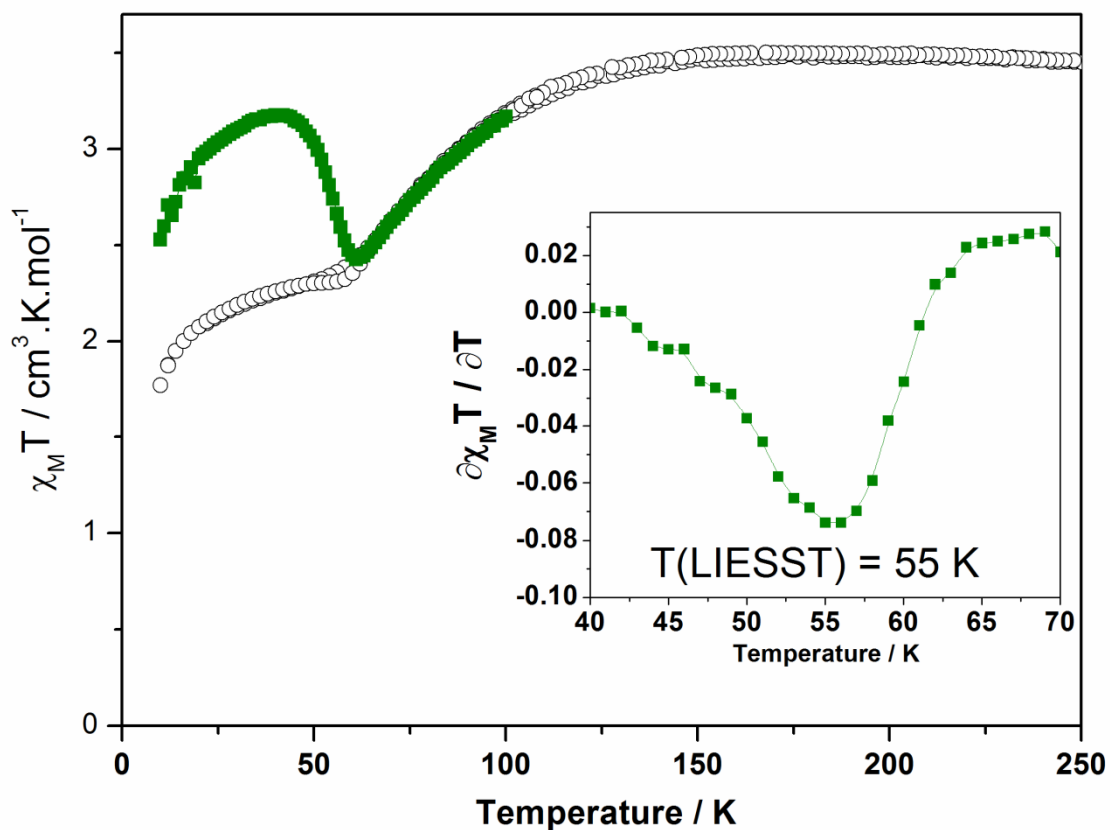


Fig. S10 Thermal behaviour of the $\chi_M T$ product of **5** before irradiation and in the dark after irradiation (■). The insert presents the derivative of the thermal $\chi_M T$ as a function of T (in the dark after irradiation); the minimum allows the determination of the $T(\text{LIESST})$ value

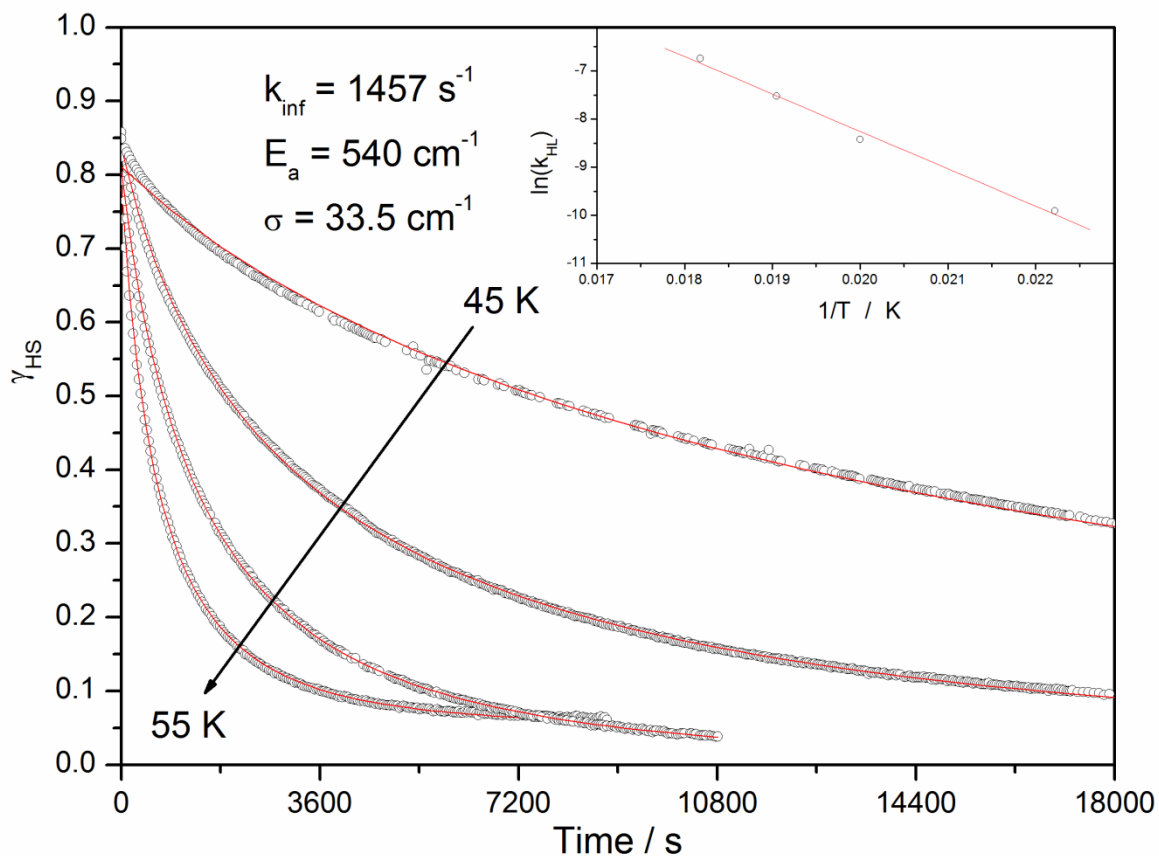


Fig. S11. Plot of the different relaxation kinetics recorded as a function of temperature (45-50 K) for **5**. The red lines are calculated using the parameters given in the text. The inset is the fit to the Arrhenius equation.

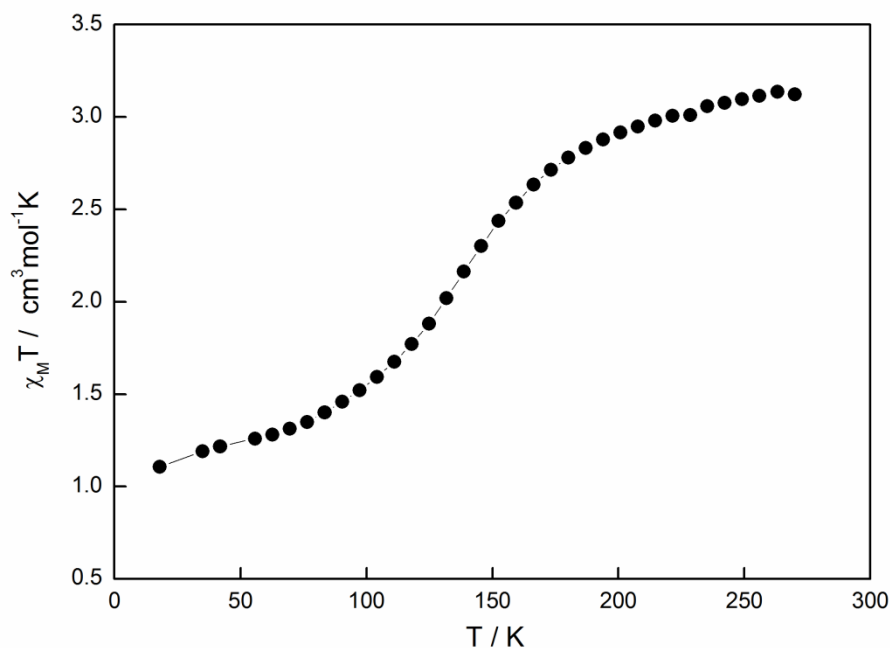


Fig. S12 Plot of $\chi_M T$ vs T for **7**, per Fe, in cooling and heating modes between 30-270 K in an applied field of 0.5 T.

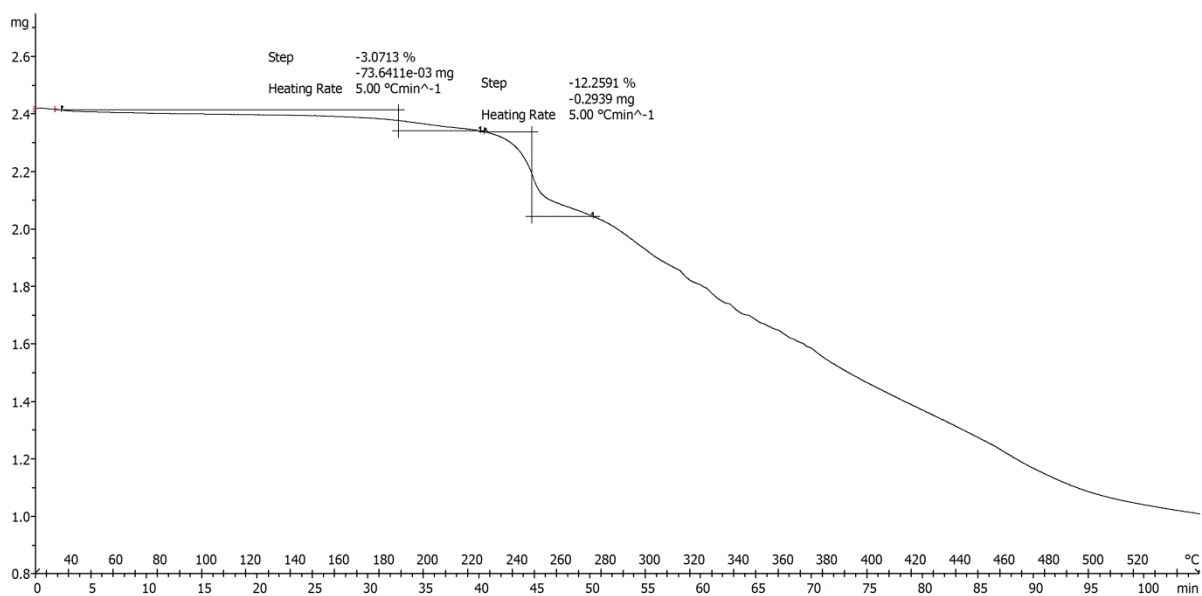


Fig. S13 Thermogravimetric Analysis (TGA) of complex **3**·1.5H₂O at a scan rate of 5 °C min⁻¹ revealing a gradual weight loss of *ca.* 3 % between 25 °C and 230 °C, an abrupt weight loss of *ca.* 12 % between 230 °C and 280 °C and a gradual weight loss after 280 °C due to complex decomposition.